ACKNOWLEDGMENT

This work was performed with the assistance of a grant from the Canadian National Research Council, A-3515. Computations were carried out with the facilities of the University of Toronto Computer Center.

NOTATION

a_i = x coordinate of stack i, m
b_i = y coordinate of stack i, m
C = average ground level sulfur dioxide concentration based on 30 min sampling time, g/m^3
d_i = exit diameter of stack i, m
H_i = effective height of stack i, m
H_{si} = height of stack i, m
k = weighting parameter defined by Equation (6)
$\mathbf{K}$ = $n \times n$ diagonal matrix defined by Equation (8)
$\mathbf{M}$ = $n \times n$ diagonal matrix defined by Equation (25)
Q_i = emission rate of stack i, g/s
$\mathbf{r}$ = search region defined by Equation (7)
T_a = air temperature, taken as 283°K
T_{si} = exit gas temperature at top of stack i, °K
u = wind velocity, m/s
V_{si} = exit gas velocity of stack i, m/s
$\mathbf{x}$ = independent variable
$\mathbf{x}^*$ = best value of $\mathbf{x}$
X_i = downwind distance from stack i, m
Y_i = crosswind distance from the plume center line of stack i, m
$\mathbf{Z}$ = $n \times n$ diagonal matrix consisting of random numbers between −1.0 and 1.0

Greek Letters

α = lower bound of $\mathbf{x}$
β = upper bound of $\mathbf{x}$
ΔH_i = plume rise from stack i, m
ϵ = amount of size reduction defined by Equation (5)
θ = wind direction measured clockwise from x axis, radian
λ = search region parameter defined by Equation (7)
ρ = radius defined by Equation (37), m
σ_{yi} = standard deviation defined by Equation (28), m
σ_{zi} = standard deviation defined by Equation (29), m
ϕ = angle defined by Equation (37), measured clockwise from x axis, radian

Superscripts

j = iteration number

LITERATURE CITED

Chen, H.T., and L. T. Fan, "Multiple Minima in a Fluidized Reactor-Heater System," *AIChE J.*, **22**, 680(1976).

Gaines, L. D., and J. L. Gaddy, "Process Optimization by Flow Sheet Optimization," *Ind. Eng. Chem. Process Design Develop.*, **15**, 206 (1976).

Hesse, R., "A Heuristic Search Procedure for Estimating a Global Solution of Nonconvex Programming Problems," *Opns. Res.*, **21**, 1267 (1973).

Heuckroth, M. W., J. L. Gaddy, and L. D. Gaines, "An Examination of the Adaptive Random Search Technique," *AIChE J.*, **22**, 744 (1976).

Luus, R., "Two-pass Method for Handling Difficult Equality Constraints in Optimization," *ibid.*, **20**, 608 (1974).

———, and T. H. I. Jaakola, "Optimization by Direct Search and Systematic Reduction of the Size of Search Region," *ibid.*, **19**, 760 (1973).

Turner, D. B., *Workbook of Atmospheric Dispersion Estimates*, Environmental Protection Agency, Office of Air Programs, Research Triangle Park, N. C. (1973).

Wang, B-C., and R. Luus, "Optimization of Nonunimodal Systems," *Intern. J. Num. Meth. Eng.*, **11**, 1235 (1977).

Manuscript received February 4, 1977; revision received January 13, and accepted February 22, 1978.

Internal Boiling and Superheating in Vaporizing Multicomponent Droplets

The vaporization and combustion of a miscible multicomponent droplet in a quiescent atmosphere is analyzed by assuming transient-diffusive transport within the droplet, quasi steady diffusive-convective transport in the gas phase, and ideal solution behavior for the mixture. Results on the vaporization of a binary droplet show that owing to the significant liquid phase diffusional resistance, the vaporization process approximately consists of an initial transient regime, an intermediate, diffusion limited, almost quasi steady regime, and a final volatility limited regime. It is further demonstrated that the entrapment of the volatile components within the rapidly heated droplet interior may lead to the initiation of either homogeneous or heterogeneous nucleation, which can result in the fragmentation of the parent droplet with the internal pressure buildup.

C. K. LAW

Department of Mechanical Engineering and Astronautical Sciences Northwestern University Evanston, Illinois 60201

SCOPE

For vaporizing multicomponent droplets without much internal circulation, the extremely slow process of liquid phase mass diffusion is rate limiting such that vaporization ceases to resemble the batch distillation process as governed by volatility differentials. The entrapment of the volatile components within the rapidly heated droplet interior may subsequently lead to homogeneous or heterogeneous nucleation and hence further atomization of the liquid droplet due to the internal pressure buildup. It is also suggested that the heterogeneously induced fragmentation is a possible mechanism in preventing the formation of large coal particle agglomerates in vaporizing coal slurry droplets. The present study aims to explore and quantify the vaporization and nucleation characteristics of a multicomponent droplet in typical combustor environments.

CONCLUSIONS AND SIGNIFICANCE

The present investigation shows that owing to the slow rate of liquid phase mass diffusion compared with that for droplet surface regression and liquid phase thermal diffusion, the vaporization process approximately consists of an initial transient regime, an intermediate, diffusion limited, almost quasi steady regime, and a final volatility limited regime which onsets when the continuously diminishing droplet size becomes comparable with the characteristic mass diffusion length. It is further demonstrated that the concept of droplet fragmentation due to the occurrence of internal homogeneous nucleation is viable; that the attainment of the limit of superheat within the droplet interior is enhanced for increased ambient temperatures, ambient pressures, and volatility differentials among the constituents; and that this concept is most suitable for application in high pressure combustors. Droplet fragmentation due to internal boiling in the presence of heterogeneous nucleation sites has also been studied and found more attractive for application in several aspects, particularly the potential on the utilization of coal slurry fuels in atmospheric combustors.

It has recently been suggested (Ivanov and Nefedov, 1965; Dryer, 1975; Jacques et al., 1975; Law, 1977) that sprays with fine droplets can be produced by emulsifying a high boiling fuel with water such that as the emulsion droplet becomes appreciably heated in the combustor, the embedded water microdroplets can be heated to the limit of superheat and subsequently explode. The disintegration of the parent droplet essentially constitutes a secondary atomization process, producing droplets of very fine sizes which can be readily vaporized. Furthermore, the violence associated with the so-called microexplosion (Ivanov and Nefedov, 1965) also disperses the secondary droplets into a large physical volume, hence producing a more uniform charge for combustion.

The primary difficulties involved with the utilization of water-in-oil emulsions are their instability from internal phase coalescence, as well as the weight and heat sink penalties associated with water addition. Whereas these difficulties either are not serious drawbacks for certain combustors or can be surmounted for others with further technological developments, an alternate mechanism to induce microexplosion, through internal superheating of a miscible, multicomponent, evaporating fuel droplet, is also possible. The concept capitalizes on the fact that the liquid phase Lewis number Le_l, representing the ratio of thermal to mass diffusion rates, is a large number. Therefore, when internal circulation is not strong such that diffusion is the dominant transport mode within the droplet, the droplet interior will be heated at a rate much faster than that with which the more volatile compounds in the inner core can be transported to the surface where they are preferentially vaporized. It is then conceivable that the volatile mixture trapped in the inner core can be heated to the limits of superheat, homogeneously nucleates, and subsequently ruptures the parent droplet with the resultant internal pressure buildup.

Whereas several analyses (Faeth, 1970; Newbold and Amundson, 1973; Law, 1976) have been performed on multicomponent droplet vaporization by assuming the internal states are maintained perpetually uniform such that the volatility differentials among the constituents are the rate limiting factors, Landis and Mills (1974) first pointed out that in the absence of internal circulation, liquid phase mass diffusion is instead the rate limiting process. Their results for the pure vaporization of a binary droplet show that after an initial transient, the internal concentrations approach almost constant profiles which persist until complete droplet consumption, and that the droplet interior can be driven to the boiling state. Hence, with suitable heterogeneous nucleation sites, internal boiling can be initiated.

Since conventional liquid fuel blends do not contain any heterogeneous nucleation sites, internal bubbling can be initiated only when the internal states have reached the limit of superheat, which requires a steeper concentration gradient, a higher droplet temperature, and is expected to be significantly more difficult to be attained than the state of boiling. The present investigation then aims to explore, and subsequently demonstrates, that with proper optimization, the limit of superheat can indeed be reached within the droplet interior. Hence, microexplosion through internal superheating is a viable concept. By studying the phenomena of interest in greater detail, we shall also show that as the droplet size diminishes, the vaporization process becomes progressively more dominated by the volatility differentials. Therefore, contrary to the results of Landis and Mills (1974), the concentration profiles do not remain at constant values towards the end of the droplet lifetime. Finally, the formulation of Landis and Mills (1974) is also generalized herein to the case of multicomponent droplet which can undergo either pure vaporization or combustion.

FORMULATION

Problem Definition

The problem analyzed is the isobaric, spherically symmetric vaporization of a droplet, initially of radius r_{so}, temperature $T_o(r)$, and consisting of N compounds characterized by their respective molar fractions $X_{io}(r)$, molecular weights W_i, specific latent heats of vaporization L_i, normal boiling temperatures T_{bi} evaluated at the normal atmospheric pressure p_b, and critical temperature T_{ci} and pressure p_{ci}, that at time $t = 0$ is introduced, and ignited in the case of combustion, in a stagnant, unbounded atmosphere. The atmosphere is characterized by its temperature T_∞, pressure p_∞, and mass fractions $Y_{i\infty}$ of its $N + 2$ species consisting of the N vaporizing species, the oxidizer gas O, and a noncondensible inert species.

For pressures not close to critical, the gas phase processes can be assumed to be quasi steady since they occur at rates much faster than those of the liquid phase processes (Law, 1976; Sirignano and Law, 1978). Hence, the relevant transport mechanisms are transient diffusion in the liquid phase and diffusion and radial convection in the gas phase. Radiative transfer is neglected owing to the small droplet sizes of interest. In the case of combustion, we shall also invoke the flame-sheet approximation, which states that the outwardly diffusing multicomponent fuel vapor F reacts stoichiometrically and completely with the inwardly diffusing oxidizer gas at an infinitesimally thin flame front located at r_f. Finally, for mathematical convenience unity, gas phase Lewis

number and conventional constant transport property assumptions will also be invoked.

The formulation then consists of descriptions for the gas and liquid phase transport processes, the interfacial phase change, and the state of the limit of superheat. These will be presented in the following.

Gas Phase Description

Explicit expressions stated in terms of the states at the gas-liquid interface have been derived (Law, 1976) for the quasi steady, spherically symmetric, convective-diffusive transport of a multicomponent gas, with or without diffusional burning confined to a flame sheet. In particular, the nondimensional expressions for the total and fractional mass vaporization rates $\hat{m}$ and ϵ_i and the amount of heat utilized for droplet heating $\hat{H}$ are, respectively, given by

$$\hat{m} = \ln\left(1 + \frac{\hat{T}_\infty - \hat{T}_s + \tilde{Y}_{0\infty}\tilde{Q}}{\tilde{L} + \hat{H}}\right) \tag{1}$$

$$\epsilon_i = Y_{is}{}^+ + (1 - Y_{Fs}{}^+)\frac{(Y_{is}{}^+ - Y_{if})}{(Y_{Fs}{}^+ - Y_{Ff})} \tag{2}$$

and

$$\hat{H} = \frac{(\hat{T}_\infty - \hat{T}_s + \tilde{L} - \tilde{Q}) + (1 + \tilde{Y}_{0\infty})[\tilde{Q} - \tilde{L}(1 - Y_{Ff})/(1 - Y_{Fs}{}^+)]}{(1 + \tilde{Y}_{0\infty})(1 - Y_{Ff})/(1 - Y_{Fs}{}^+) - 1} \tag{3}$$

where $\hat{m} = m/(4\pi\rho_g D_g r_s)$, $\epsilon_i = m_i/m$, $\tilde{L} = \Sigma\epsilon_i\hat{L}_i$, $\tilde{Q} = \Sigma\epsilon_i\hat{Q}_i$, $\tilde{Y}_\infty = Y_{0\infty}/\Sigma\epsilon_i V_i$, $Y_F = \Sigma Y_i$, $\hat{T} = C_g T/L_r$, $\hat{L}_i = L_i/L_r$, $\hat{Q}_i = Q_i/L_r$, $\hat{H} = H/L_r$, L_r is a reference latent heat of vaporization, and for convenience we can assume the value of unity in the system of units adopted. The summation operation is to be performed over all of the vaporizing species. The problem has also been formulated in such a generalized manner that the results specialize to combustion by setting $Y_{if} = 0$ and to pure vaporization by setting $Y_{0\infty} = 0$ and $Y_{if} = Y_{i\infty}$.

Liquid Phase Description

The unsteady liquid phase heat and mass diffusion are governed by

$$\frac{\partial T}{\partial t} = \frac{\alpha_l}{r^2}\frac{\partial}{\partial r}\left(r^2\frac{\partial T}{\partial r}\right) \tag{4}$$

$$\frac{\partial Y_i}{\partial t} = \frac{D_l}{r^2}\frac{\partial}{\partial r}\left(r^2\frac{\partial Y_i}{\partial r}\right) \tag{5}$$

Since one of the liquid phase boundaries is continuously regressing, solutions for Equations (4) and (5) can be facilitated by fixing the droplet surface at unity and by moving the upper limit in time from a finite to an infinite value through the transformations

$$\sigma = \frac{r}{r_s(t)} \quad \text{and} \quad \tau = \int_o^t \frac{\alpha_l}{r_s^2(t')}dt' \tag{6}$$

Using Equation (6), Equations (4) and (5) are, respectively, transformed to

$$\frac{\partial T}{\partial \tau} = \frac{1}{\sigma^2}\frac{\partial}{\partial \sigma}\left(\sigma^2\frac{\partial T}{\partial \sigma}\right) - K_1\hat{m}\sigma\frac{\partial T}{\partial \sigma} \tag{7}$$

$$\frac{\partial Y_i}{\partial \tau} = \frac{1}{Le_l\sigma^2}\frac{\partial}{\partial \sigma}\left(\sigma^2\frac{\partial Y_i}{\partial \sigma}\right) - K_1\hat{m}\sigma\frac{\partial Y_i}{\partial \sigma} \tag{8}$$

which are to be solved with the initial and boundary conditions

$$T(\sigma, 0) = T_o(\sigma), \quad Y_i(\sigma, 0) = Y_{io}(\sigma) \tag{9}$$

$$(\partial T/\partial\sigma)_{\sigma=0} = 0, \quad (\partial Y_i/\partial\sigma)_{\sigma=0} = 0 \tag{10}$$

$$(\partial T/\partial\sigma)_{\sigma=1} = K_2\hat{m}(\hat{H} - \tilde{L}) \tag{11}$$

$$(\partial Y_i/\partial\sigma)_{\sigma=1} = Le_l K_1\hat{m}(Y_{is}{}^- - \epsilon_i) \tag{12}$$

where $K_1 = (\lambda_g C_l)/(\lambda_l C_g)$, $K_2 = \lambda_g/\lambda_l$, and the identity

$$\hat{m} = -(\rho_l C_g/2\lambda_g)dr_s^2/dt \tag{13}$$

has been used. Equations (11) and (12) represent energy and species conservations at the interface.

Hence, with $\hat{m}$, ϵ_i, and $\hat{H}$ given by Equations (1) to (3), and using the phase change description of Equation (16) which relates $Y_{is}{}^+$ and $Y_{is}{}^-$, $T(\sigma, \tau)$ and $Y_i(\sigma, \tau)$ can be solved from Equations (7) to (12). The instantaneous droplet size is obtained by integrating Equation (13), yielding

$$\hat{r}_s^2(\tau) = \exp\left[-2K_1\int_o^\tau \hat{m}(\tau')d\tau'\right] \tag{14}$$

where $\hat{r}_s = r_s/r_{so}$. Finally, when we invert Equation (6), the nondimensional physical time $\hat{t} = (\alpha_l/r_{so}^2)t$ is

$$\hat{t} = \int_o^\tau \hat{r}_s^2(\tau')d\tau' \tag{15}$$

with $\hat{r}_s^2(\tau)$ given by Equation (14).

Phase Change Description

Since for a volatile liquid the phase change process occurs at rates much faster than the gas phase transport processes, the vapor concentration at the droplet surface can be considered to be saturated. By further assuming that the liquid behaves as an ideal mixture, Raoult's law states that

$$X_{is}{}^+ = X_{is}{}^-\left(\frac{p_b}{p_\infty}\right)\exp\left[\left(\frac{L_i}{R_i}\right)\left(\frac{1}{T_{bi}} - \frac{1}{T_s}\right)\right] \tag{16}$$

where the molar and mass fractions are related through

$$Y_i = \frac{X_i W_i}{\Sigma X_i W_i} \tag{17}$$

The Limit of Superheat

Skripov (1974) and Apfel (1971) have measured, for a variety of pure substances, the limits of superheat as a function of pressure, which were shown (Eberhart and Schnyder, 1973) to be approximately correlatable by a modified equation of state. This correlation, however, is somewhat inconvenient to use owing to the implicitness with which the variables are related. We have instead found that the available data can be quite satisfactorily correlated by (Figure 1)

$$(1 - T_{Li}/T_{ci}) = 0.111(1 - p/p_{ci})^{0.858} \tag{18}$$

which provides an explicit relation between the variables. The standard and maximum deviations in the fitting are 0.005651 and 0.01255, respectively.

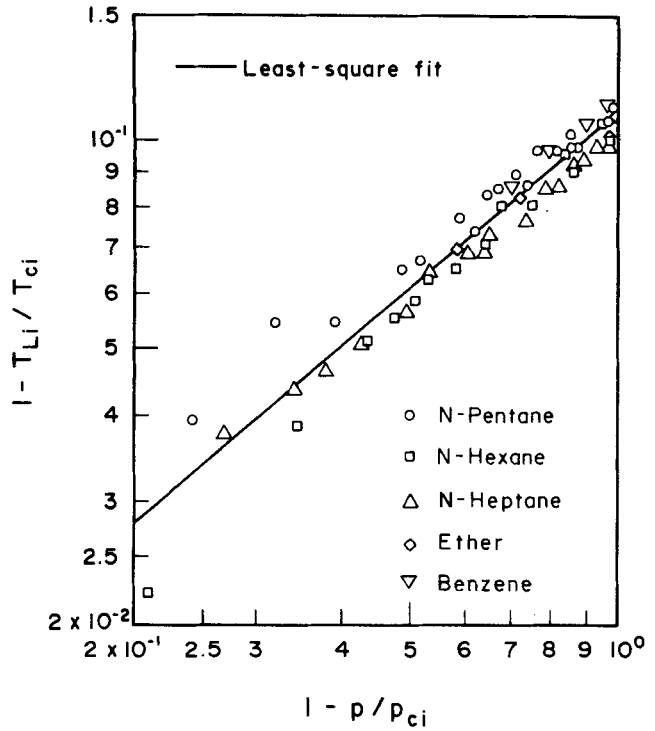

Fig. 1. Experimental and fitted limits of superheat for pure liquids as a function of pressure.

For small values of (p/p_{ci}), Equation (18) can be expanded, giving

$$(T_{Li}/T_{ci}) \simeq 0.889 + 0.0952(p/p_{ci}) \qquad (19)$$

which shows that in this limit (T_{Li}/T_{ci}) depends linearly, but very insensitively, on (p/p_{ci}). In particular, for vanishing (p/p_{ci}), which is approximately the case for many liquids at 1 atm, (T_{Li}/T_{ci}) is a constant equal to 0.889.

Measurements on the limit of superheat of mixtures which exhibit close ideal solution behavior show an approximate linear variation with the liquid molar fraction (Blander and Katz, 1975); namely

$$\tilde{T}_L = \Sigma T_{Li} X_i \qquad (20)$$

Hence, combining Equations (18) and (20), we can estimate the limit of superheat for a given mixture composition at a given pressure. It may also be noted that since the sizes of the fuel droplets of interest are typically of the order of 100 μm and hence are not small, the internal pressure is essentially the same as that of the ambiance.

This completes the description of the model. If we know the instantaneous concentration distributions within the droplet, the limits of superheat $\tilde{T}_L(\sigma, \tau)$ can be computed and compared with the droplet temperature $T(\sigma, \tau)$. The instant at which $\tilde{T}_L(\sigma, \tau) = T(\sigma, \tau)$ is satisfied somewhere within the droplet signifies the onset of internal bubbling due to homogeneous nucleation and is approximately identified as the state when microexplosion of the droplet occurs.

RESULTS AND DISCUSSIONS

Equations (7) to (12) were numerically integrated using the Crank-Nicolson technique. The radial mesh size was taken to be 0.05. Accuracy in the numerical scheme was further assured by decreasing the mesh size by at least a factor of two and noticing essentially no change in the computed results.

All the results to be presented in the following are for the pure vaporization of a binary droplet, with $T_o(\sigma) = 300°K$ and $X_{io}(\sigma) = 0.5$, in a constant environment devoid of any fuel vapor. The gas phase specific heat is taken to be that of the fuel vapor at about 1 500°K, $C_g = 1$ cal/g-°K, since fuel vapor is the only species which is transported through convection. Further, noting that $C_l \simeq C_g$, and that λ_g/λ_l is typically between 0.1 and 0.3, we have used $K_1 = K_2 = 0.2$. The liquid phase properties are representative of those of alkanes between T_o and the boiling point, whereas λ_g is that of air between 1 000° to 2 000°K.

Figure 2 shows the molar concentration profiles of decane in a decane-dodecane droplet which is undergoing pure vaporization in a $T_\infty = 2\,000°K$, $p_\infty = 1$ atm environment. The curves are also plotted as functions of Le_l and $M = 1 - \hat{r}_s^3$, which represents the fractional amount of the original droplet mass vaporized and for the present study appears to be a more meaningful indication of the progress in the vaporization process than either the physical time $\hat{t}$ or the transformed time τ.

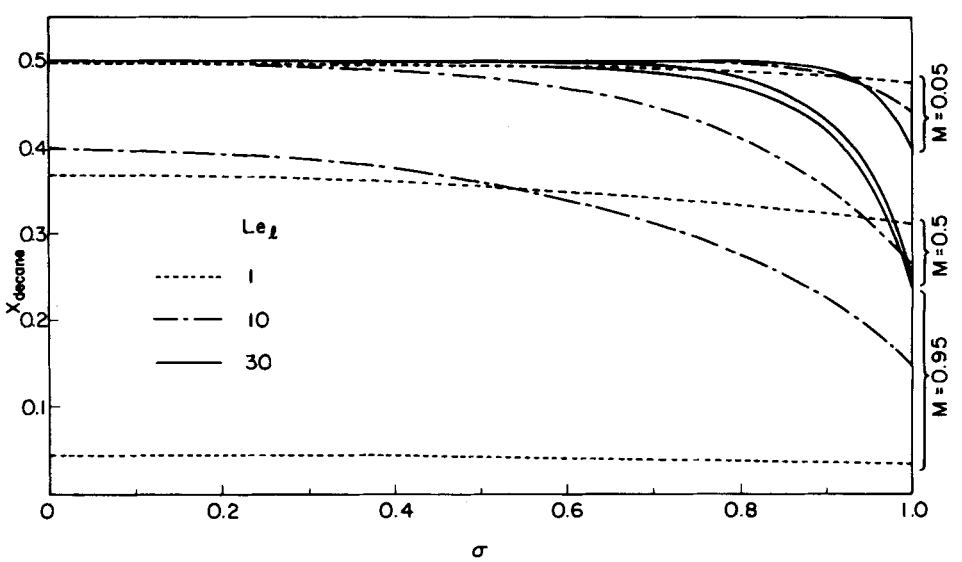

Fig. 2. Concentration profiles of decane for a decane-dodecane droplet vaporizing in a 2 000°K, 1 atm environment.

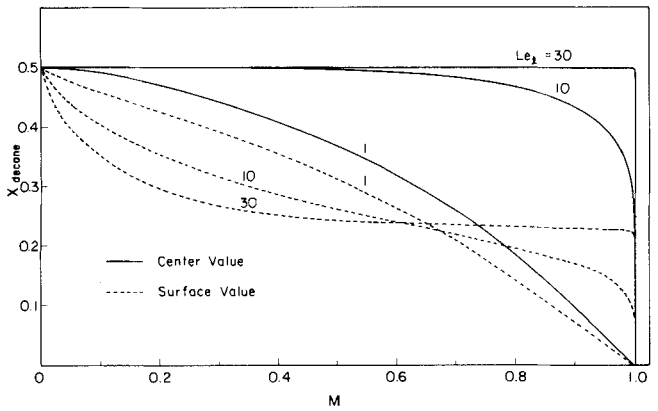

Fig. 3. Surface and center values of decane concentration as a function of M for a decane-dodecane droplet vaporizing in a 2 000°K, 1 atm environment.

Since the presence of internal circulation diminishes Le_l owing to the increased convective transport which is equally efficient for both heat and mass, effects caused by the varying degrees of internal circulation can be simulated by decreasing Le_l. Hence, results are presented both for $Le_l = 30$, which is representative of typical liquid fuels, and for smaller values of Le_l. In the limit of convection dominated transport, $Le_l \rightarrow 1$.

Figure 2 shows that the concentration profiles are qualitatively influenced by Le_l. When mass diffusional resistance is significant, at $Le_l = 30$, a steep concentration gradient exists near the droplet surface, although as σ decreases, an almost uniform state is rapidly approached. Comparing the $M = 0.5$ and 0.95 cases also shows that an approximately constant profile exists for a significant portion of the droplet lifetime. These diffusion limited characteristics gradually disappear as Le_l decreases until for $Le_l = 1$, at which heat and mass transport are equally efficient, the concentration gradient is gentle and uniform throughout the droplet. Furthermore, since decane can now be more readily brought to the surface where it is preferentially vaporized owing to its higher volatility, its concentration within the droplet is rapidly depleted.

The above observations are further illustrated in Figure 3, where the surface and center values of the molar fraction of decane are plotted vs. M. It is of particular interest to note that for $Le_l = 30$, the vaporization process consists of three regimes. During the initial transient regime, the decane concentration near the surface is rapidly depleted owing to its volatility, although its value in the inner core is practically undisturbed. Subsequently, an intermediate, mass diffusion limited, almost quasi steady regime exists during which the species are transported to, and exposed at, the regressing surface at approximately constant rates. For large Le_l, this steady period persists until almost complete droplet consumption. However, towards the end of the droplet lifetime, a volatility limited regime exists during which the more volatile component becomes rapidly depleted from the entire droplet composition. The vaporization characteristics now resemble those of the rapid mixing model (Faeth, 1970; Newbold and Amundson, 1973; Law, 1976). This result is physically realistic because as the droplet vaporizes, its size will eventually become comparable with the characteristic diffusion length. Then, diffusional transport is significantly enhanced, the concentrations are almost perpetually uniformized, and hence volatility differentials limit the vaporization process.

The droplet size at which this volatility limited regime becomes important can be estimated as follows. First

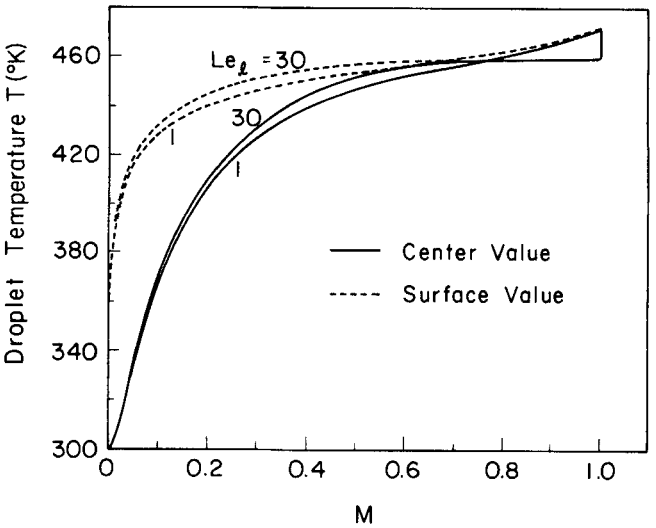

Fig. 4. Surface and center values of temperature as a function of M for a decane-dodecane droplet vaporizing in a 2 000°K, 1 atm environment.

note that since $\hat{m}$ does not vary significantly except during the very initial period (Law and Sirignano, 1977), the variation of the droplet size can be estimated by integrating Equation (13) with an average $\hat{m}$, $<\hat{m}>$. This yields

$$r_s^2 = r_{so}^2 - (2\lambda_g <\hat{m}>/\rho_l C_g)t \qquad (21)$$

Furthermore, since the characteristic diffusion length Λ_l is

$$\Lambda_l = (D_l t)^{1/2} \qquad (22)$$

we have, after eliminating t from Equations (21) and (22)

$$(\Lambda_l/r_s) = [(\hat{r}_s^{-2} - 1)/(2K_1 <\hat{m}> Le_l)]^{1/2} \qquad (23)$$

Therefore, diffusional transport is expected to be significantly enhanced when $(\Lambda_l/r_s) = 1$, or

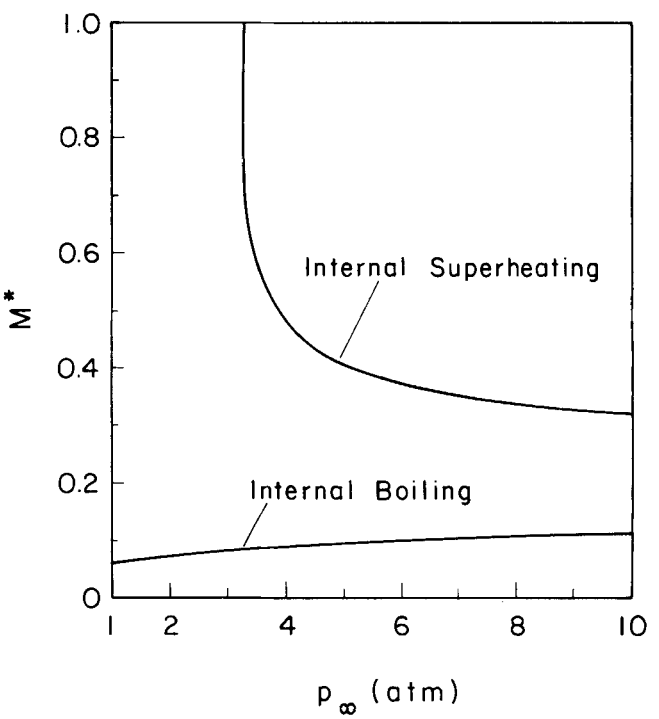

Fig. 5. Amount of droplet mass vaporized at the onset of internal bubbling as a function of ambient pressure for a heptane-hexadecane droplet vaporizing in a 2 000°K environment.

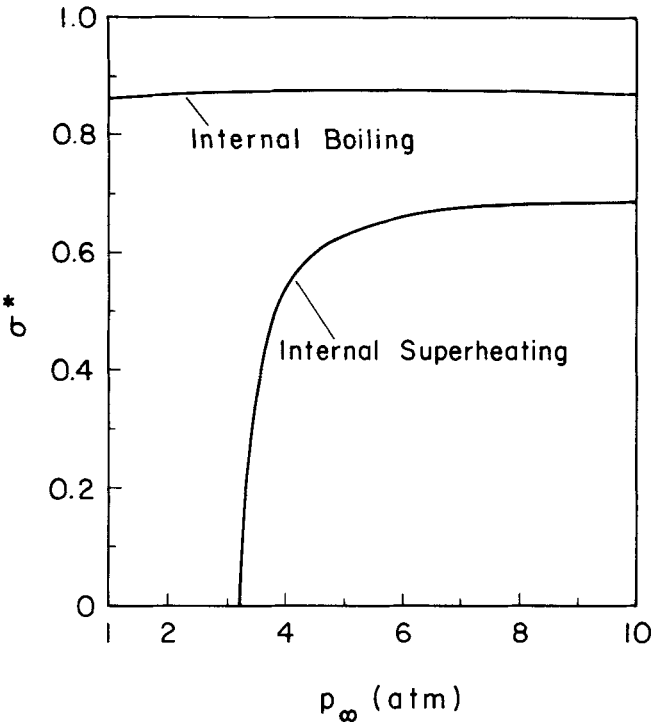

Fig. 6. Location within droplet where internal bubbling initiates as a function of ambient pressure for a heptane-hexadecane droplet vaporizing in a 2 000°K environment.

$$M = 1 - (1 + 2K_1 < \hat{m} > Le_l)^{-3/2} \qquad (24)$$

Since $2K_1 = O(1)$, Equation (24) shows that efficient diffusional transport onsets early in the droplet lifetime for $< \hat{m} > Le_l = O(1)$ or less but occurs only towards the end for $< \hat{m} > Le_l >> 1$. For the present case $< \hat{m} > = O(1)$, Figure 3 shows that for $Le_l = 30$, this volatility limited regime is distinct and occurs when $M \rightarrow 1$.

Figure 3 further shows that the three regimes identified for $Le_l = 30$ become less distinct as Le_l decreases. Hence, for $Le_l = 10$, the quasi steady regime ceases to be distinct, whereas, for $Le_l = 1$, the entire vaporization process is transient and volatility limited.

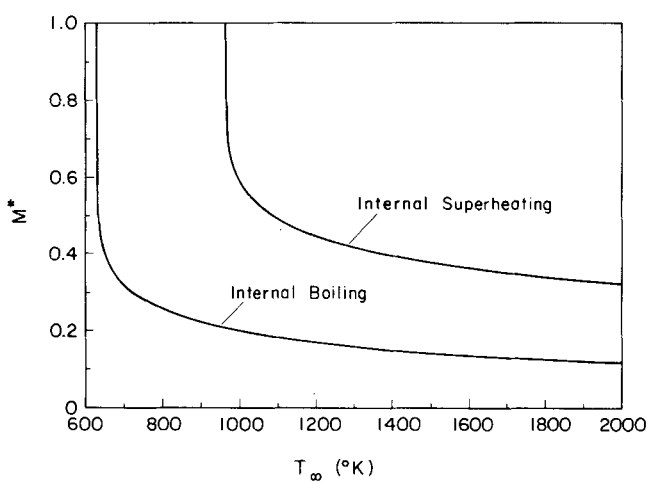

Fig. 7. Amount of droplet mass vaporized at the onset of internal bubbling as a function of ambient temperature for a heptane-hexadecane droplet vaporizing in a 10 atm environment.

Figure 4 shows the temporal variations of the surface and center values of the droplet temperature. Since liquid phase heat conduction is an efficient process regardless of the existence of internal circulation (Law and Sirignano, 1977), Figure 4 shows that the temperature histories are qualitatively similar for both the high and low Le_l values, except for the existence of the final, volatility limited regime at $Le_l = 30$, during which the droplet temperature rapidly increases to approach the wet-bulb value of the less volatile component.

We next present results on the possible attainment of the limit of superheat within the droplet interior as a function of the ambient temperature and pressure, with $Le_l = 30$. The binary components selected for study are heptane and hexadecane, whose volatilities are respectively representative of gasoline, a volatile fuel, and diesel, a nonvolatile fuel. These are selected because the attainment of superheating can be facilitated by utilizing components with large volatility differentials. The less volatile component, which has a larger concentration at the droplet surface and a higher boiling point, is needed to achieve a higher droplet temperature, whereas the more volatile component, which is more concentrated in the interior and also has a lower limit of superheat, is used to suppress the concentration-weighted limit of superheat, $\tilde{T}_L$.

The two important parameters characterizing the phenomenon are the time and location the limit of superheat is first attained. Obviously, to maximize the benefits of microexplosion caused by internal bubbling, this event should occur deep within the droplet and early in the droplet lifetime.

Denoting the state at which internal bubbling initiates by the superscript "*", Figure 5 shows M^* as a function of p_∞, with $T_\infty = 2\,000$°K. It is seen that increasing p_∞ enhances the occurrence of internal bubbling. This is because as p_∞ increases, the boiling point of the fuel, and hence the droplet temperature, increases at a much faster rate than that for the limit of superheat. Figure 5 also shows that a minimum p_∞ exists below which internal bubbling cannot occur. For pressures higher than those in this critical regime, internal bubbling occurs when about 30 to 40% of the droplet mass has been vaporized. The above observations suggest that the concept of microexplosion induced by internal superheating is more suitable for application in high pressure combustors, for example, the diesel engine.

Figure 6 shows the location σ^*, where the limit of superheat is first reached within the droplet. It is seen that except in the critical regime of 3 to 4 atm, σ^* is between 0.6 to 0.7, and hence $(r^*)^3$ is between 0.2 to 0.35. Therefore, from a mass point of view, bubbling can be considered to occur quite deep within the droplet. It is also significant to note that although the onset of bubbling is relatively delayed in the critical regime, it occurs deep within the droplet such that the microexplosive effects are maximized.

Figure 7 shows M^* as a function of T_∞, with $p_\infty = 10$ atm. As expected, M^* decreases with increasing T_∞. A minimum T_∞ also exists below which internal bubbling is not possible.

It is also of interest to investigate the characteristics of internal bubbling caused by heterogeneous nucleation, assuming that some heterogeneous nucleation sites are present within the droplet. This scheme appears to be more attractive than microexplosion through internal superheating in several aspects. Since heterogeneous nucleation can be attained much more readily than homogeneous nucleation, the concept of microexplosion can now be applied to fuel blends with smaller volatility

differentials and to combustor environments with lower temperatures and pressures. In fact, Figure 5 shows that M^* actually slightly decreases with decreasing p_∞, hence making its utilization particularly attractive in atmospheric combustors, for example, the industrial and domestic furnaces. Furthermore, with internal boiling, the droplet interior temperature is limited to the local boiling point of the fuel mixture; hence the intensity of liquid phase pyrolysis, and subsequently the extent of soot formation, may be substantially lessened. Finally, since a less steep concentration gradient is required, some degree of internal circulation, which is usually unavoidable in realistic situations, can also be tolerated.

Figures 5 and 7 also show that internal bubbling can be initiated early in the droplet lifetime, which is beneficial for enhanced atomization effects; although due to the smaller internal vapor pressure buildup and the fact that nucleation now occurs closer to the surface (Figure 6), the microexplosive event is expected to be less violent and hence less effective. The primary drawback of this scheme, however, is the need to introduce heterogeneous nucleation sites. Since these sites are naturally present in droplets of coal-dust-in-oil slurries, the potential of their utilization in boilers and furnaces as a measure to conserve fuel oil appears more attractive. It is also of significance to note that without the postulated heterogeneously induced internal bubbling and hence droplet fragmentation, it is conceivable that the coal particles within the slurry droplet will become progressively more concentrated as the much more volatile liquid components are vaporized. Eventually, a large coal particle agglomerate will be formed, and, depending on the remaining residence time in the combustor, incomplete combustion of this agglomerate may occur. Then not only are the chemical energy of the coal particles not utilized, but a large amount of smoke is also exhausted. Even if complete combustion is possible, the sizes of the ash particles produced may also be larger than desired. Fortunately, the present study indicates that this is not likely to be the case.

ACKNOWLEDGMENT

This research was sponsored by the Division of Fossil Energy Research, Department of Energy under Grant EF-77-G-01-2741. The author also wishes to express his sincere appreciation to H. K. Law for her able assistance with the numerical work.

NOTATION

C = specific heat at constant pressure
D = mass diffusivity
H = energy used for droplet heating per unit mass of fuel vaporized
K_1, K_2 = $(\lambda_g C_l)/(\lambda_l C_g)$, λ_g/λ_l
L_i = specific latent heat of vaporization
Le = Lewis number
m_i = mass evaporation rate of i
$<\hat{m}>$ = average nondimensional mass evaporation rate
M = fraction of mass vaporized, $1 - \hat{r}_s^3$
p = pressure
Q_i = heat of reaction per unit mass of i reacted
r = radial distance
$\hat{r}$ = r_s/r_{so}
R_i = gas constant of i
t = time
T = temperature
T_{Li} = limit of superheat of i
W_i = molecular weight of i
X, Y = molar and mass fraction, respectively

Greek Letters

α = thermal diffusivity
ϵ_i = fractional mass vaporization rate, m_i/m
λ = thermal conductivity
Λ = characteristic length for mass diffusion
τ = transformed time, Equation (6)
ν_i = stoichiometric mass ratio of oxidizer to i
ρ = density
σ = transformed radial distance, $r/r_s(t)$

Subscripts

b = boiling state
c = critical state
f = flame
F = all of the fuel species
g = gas phase
i = index for fuel species
l = liquid phase
o = initial state
O = oxidizer
s = droplet surface
s^+, s^- = gas and liquid side of droplet surface
∞ = ambiance

Superscripts

$\sim$ = species weighted quantity
$\wedge$ = nondimensionalized quantity
$*$ = state of internal bubbling

LITERATURE CITED

Apfel, R. E., "A Novel Technique for Measuring the Strength of Liquids," *J. Acoust. Soc. Am.*, **49**, 145 (1971).

Blander, M., and J. L. Katz, "Bubble Nucleation in Liquids," *AIChE J.*, **21**, 833 (1975).

Dryer, F. L., "Fundamental Concepts on the Use of Emulsions as Fuels," paper presented at the Joint Spring Meeting of the Central and Western States Section of the Combustion Institute, San Antonio, Tex. (1975).

Eberhart, J. G., and H. C. Schnyders, "Application of the Mechanical Stability Condition to the Prediction of the Limit of Superheat for Normal Alkanes, Ether and Water," *J. Phys. Chem.*, 77, 2730 (1973).

Faeth, G. M., "Combustion Characteristics of Blended Monopropellant Droplets," *AIAA Paper No. 70-7* (1970).

Ivanov, V. M., and P. I. Nefedov, "Experimental Investigation of the Combustion Processes in Natural and Emulsified Fuels," *NASA TT F-258* (1965).

Jacques, M. T., J. B. Jorden, and A. Williams, "The Combustion of Emulsions of Water and Fuel Oil," *Deuxiene Symposium European sur la Combustion, The Combustion Institute*, 397-402 (1975).

Landis, R. B., and A. F. Mills, "Effects of Internal Diffusional Resistance on the Vaporization of Binary Droplets," paper B7.9, 5th International Heat Transfer Conference, Tokyo, Japan (1974).

Law, C. K., "Multicomponent Droplet Combustion with Rapid Internal Mixing," *Combust. Flame*, **26**, 219 (1976).

———, "A Model for the Combustion of Oil/Water Emulsion Droplets," *Combust. Sci. Technol.*, **17**, 29 (1977).

———, and W. A. Sirignano, "Unsteady Droplet Combustion with Droplet Heating. II. Conduction Limit," *Combust. Flame*, **28**, 175 (1977).

Newbold, F. R., and N. R. Amundson, "A Model for Evaporation of a Multicomponent Droplet," *AIChE J.*, **19**, 22 (1973).

Sirignano, W. A., and C. K. Law, "A Review of Transient Heating and Liquid-Phase Mass Diffusion in Fuel Droplet Vaporization," to appear in *ACS Advan. Chem. Ser.* (1978).

Skripov, V. P., *Metastable Liquids*, Wiley, New York (1974).

Manuscript received November 9, 1977; revision received March 8, and accepted March 27, 1978.